OPTOELECTRONICS AND ADVANCED MATERIALS – RAPID COMMUNICATIONS Vol. 1, No. 11, November 2007, p. 549 - 553

Performance of optical displacement sensor using a pair type bundled fiber from a theoretical and experimental perspective

M. YASIN*, S. W. HARUN[a], H. A. ABDUL-RASHID[b], KUSMINARTO[c], KARYONO[c], A. H. ZAIDAN, H. AHMAD[d]
Department of Physics, Faculty of Mathematics and Natural Science, Airlangga University, Surabaya 60115, Indonesia
[a]Department of Electrical Engineering, Faculty of Engineering, University of Malaya 50603 Kuala Lumpur, Malaysia
[b]Faculty of Engineering, Multimedia University, 63100 Cyberjaya, Malaysia
[c]Department of Physics, Faculty of Mathematics and Natural Science, Gadjah Mada University, Yogyakarta, Indonesia
[d]Photonics Laboratory, Department of Physics, University of Malaya, 50603 Kuala Lumpur, Malaysia

An optical displacement sensor using a pair type bundled fiber is investigated from both the theoretical and experiment perspectives. The theoretical analysis uses an electromagnetic Gaussian beam approach to determine a transfer function of the sensor. The displacement between a flat mirror and the bundled fiber end is measured using an intensity modulation technique. The sensor has two operating ranges with a good linearity; namely the front slope and back slope. On the front slope the sensitivities are obtained at 1.71 and 1.0 mW/μm for the theoretical and experimental approaches respectively while on the back slope the sensitivities are 0.38 and 0.22 mW/μm for theoretical and experimental approaches respectively. This discrepancy in theoretical and experimental values is due to neglecting the effect of Gaussian beam truncation in our simple theoretical model. The front slope is highly sensitive and useful for close distance targets while the back slope is less sensitive and useful for large displacement movements.

(Received October 3, 2007; accepted October 31, 2007)

Keywords: Fiber-optic displacement sensor, A pair bundled fiber, Paraxial Gaussian beams

1. Introduction

Multimode plastic fibers are in great demand for the transmission and processing of optical signals in optical fiber communication systems. They are also widely used in sensing applications because they exhibit better signal coupling, larger core radii, and a higher numerical aperture as well as being able to receive the maximum reflected light from the target [1-2]. As such, a multimode plastic bundle fiber is extremely well suited for displacement sensor applications, which is seen to play an increasingly larger role in a broad range of industrial, military and medical applications [3-5].

Two primary advantages of fiber optic displacement sensors include the potential for extremely accurate non-contact sensing and the possibility of incorporating the optical sensors permanently into composite structures. Fiber-optic sensors raised a great interest due to their inherent simplicity, small size, mobility, wide frequency capability, extremely low displacement detection limit [6] and ability to perform non-contacting measurement. In this paper, a fiber bundle based optical displacement sensor is investigated from a theoretical and experimental perspective. The sensor uses a pair type of bundled fibers in conjunction with an intensity modulation technique to measure the displacement between mirror and bundled fiber's end.

2. Theoretical analysis

The basic set-up for a displacement sensor consists of a modulated light source, detector and a Y branched bundled fiber and a planar mirror. The Y branched bundled fiber consists of a pair of transmitting and receiving fibers as shown in Fig. 1. Displacement is measured by comparing the power of the reflected light, which is coupled back into a receiving fiber from a mirror with a portion of power emitted by the same light source. The amount of light that returns to the detector depends on the distance between the end of the bundled fiber and the mirroring surface being monitored. In order to analyze the displacement sensing characteristic theoretically, the following assumptions are made;

(i) The bundled fiber in front of the mirror is modeled as a set of two independent parallel equal fibers in contact with each other with no space left between them. Both the transmitting and receiving fibers are assumed to have perfectly circular cross sections with area S_a and radius w_a as shown in Fig. 1.

(ii) The light leaving the transmitting fiber is represented by a perfectly symmetrical cone with divergence angle θ_a, and vertex 0 located at a distance z_a inside the fiber, as shown in Fig. 2.

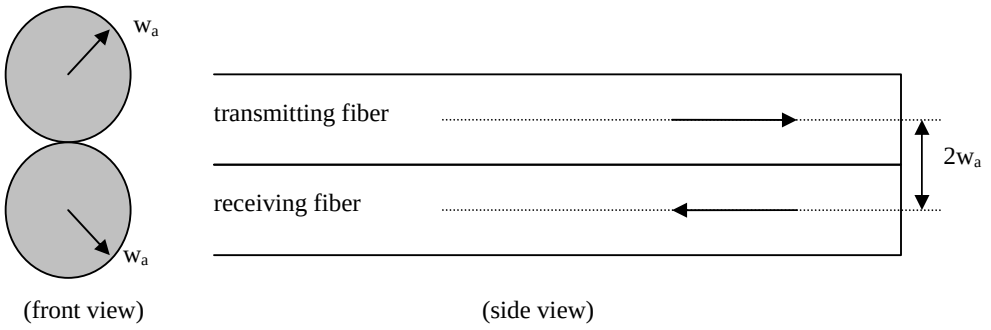

Fig. 1. Front and side views of the transmitting and receiving bundled fiber ends.

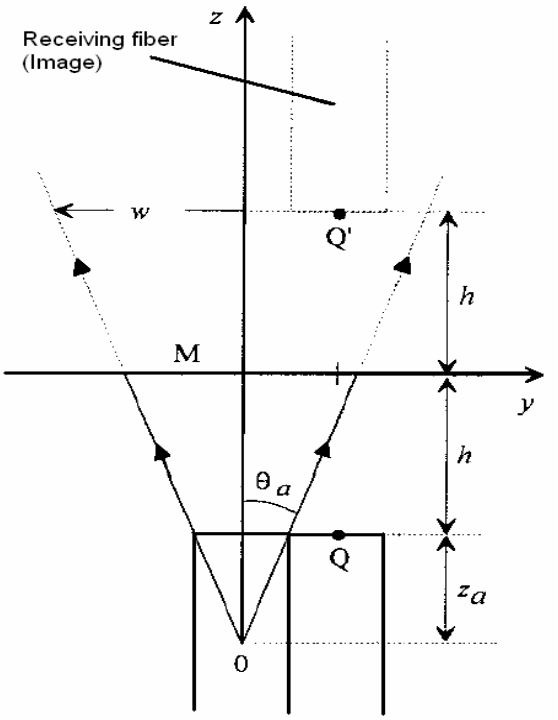

Fig. 2. Cone of light exiting the transmitting fiber. The cone is extended beyond the mirror and the image position of the receiving end is analyzed.

In order to evaluate the amount of light collected by the receiving fiber, the light cone is extended beyond the mirror as shown in Fig. 2 and the image position at the receiving end is analyzed. A z-coordinate is introduced which is aligned to the emitted light cone axis beginning at 0 and extending beyond the mirroring surface. The coordinate of the center point in the receiving fiber end is designated as Q' as shown in Fig. 2 and is represented by;

$$Q'\begin{cases} y = 2w_a \\ z = z_a + 2h \end{cases} \tag{1}$$

where h is the distance being monitored.

The theoretical approach is based on the electromagnetic theory of paraxial Gaussian beams, which is used to derive the transfer function that is dependent on the variance of the optical power collected by the receiving fiber bundle [7]. This approach describes the light leaving the transmitting fiber bundle as a paraxial beam with a Gaussian profile. The irradiance of the emitted light decreases radially over the beam cross-sections, obeying an exponential law according to

$$I(r,z) = \frac{2P_E}{\pi w^2(z)} \exp\left(-\frac{2r^2}{w^2(z)}\right) \tag{2}$$

where r is the radial coordinate, z is the longitudinal coordinate and radius $w(z) = w_0\sqrt{1+(z/z_R)^2}$ is a measure of the beam width whose dependence is on z . The constants ω_0 and z_R are the waist radius and Rayleigh range respectively and their relationship is given by;

$$\pi w_0^{\,2} = \lambda z_R \tag{3}$$

In the case of the points situated in the far-field zone ($z >> z_R$), the beam resembles a spherical wave confined within a cone as depicted in Fig. 2. The cone is characterized by a divergence angle given by:

$$\theta_a \approx \tan\theta_a = \frac{w(z)}{z} = \frac{w_0}{z_R} = \frac{\lambda}{\pi w_0} \tag{4}$$

and the irradiance function can be simplified as;

$$I(r,z) = \frac{2P_E}{z^2\pi\theta_a^{\,2}} \exp\left(-\frac{2r^2}{\theta_a^{\,2}z^2}\right) \tag{5}$$

The optical power collected by the receiving fiber is evaluated by integrating I(r,z) over the fiber end surface S_a as shown below:

$$P(z) = \int_{S_a} I(r,z)dS \,. \tag{6}$$

We assume that the irradiance I(r,z) is approximately constant across the receiving surface with area $S_a = \pi w_a^{\,2}$, and equal to its value at the center of the receiving fiber (point Q') where $r = 2w_a \approx 2\theta_a z_a$. In this case, we obtain

$$P = IS_a = \frac{2P_E}{\zeta^2}\exp\left(-\frac{8}{\zeta^2}\right) \tag{7}$$

where

$$\zeta = \frac{z}{z_a} = 1 + \frac{2h}{z_a} = 1 + 2h_N \tag{8}$$

and h_N is a normalized distance. By analyzing $dP/d\zeta = 0$, the collected power reaches its maximum value $P_{\max} = P_E/(4e)$ value when $\zeta = \sqrt{8}$ (i.e., $h_N = 0.9142$) the collected power reaches its maximum $P_{\max} = P_E/(4e)$ value. Taking this into account, we may rewrite (Eq. 7) in normalized form $P_N = P/P_{\max}$ as

$$P_N = \frac{8}{\zeta^2}\exp\left(1 - \frac{8}{\zeta^2}\right) \tag{9}$$

A normalized distance can be evaluated using Eq. 4. and Fig. 2. If, r = 0.5 mm, λ = 633 nm and w_0 = 0.46 mm, z_a is calculated to be 1141 mm. By using $h_N = h/z_a$, we obtain $h_N = h/1141mm$, where h is a displacement, which has moved in 50 μm steps in the experiment. The sensor sensitivity is evaluated by deriving of P_N with respect to h_N

$$S = \frac{\partial P_N}{\partial h_N} \tag{10}$$

Making use of Eq. 9, we get;

$$S = 2\frac{\partial}{\partial \zeta}P_N = \frac{4}{\pi}\left(\frac{8}{\zeta^2} - 1\right)P_N(\zeta) \tag{11}$$

3. Experiment

Fig. 3 shows the experimental set-up of the displacement sensor using an intensity modulation technique. It consists of a light source, a fiber optic probe, a flat mirror and a silicon detector. The light source is a 633 nm He-Ne laser, which is modulated externally by chopper with a frequency of 200 Hz. The fiber probe is a pair type bundled plastic fiber with a length of 2 m and a core diameter of 1mm. The modulated light is launched into the transmitting fiber and then radiates to the mirror. The light reflected from the mirror is transmitted through the receiving fiber to a silicon detector. The photon energy collected by the detector is converted into a voltage by a digital voltmeter. The displacement of mirror causes a change in the received light intensity, which is a function of displacement between the fiber probe and mirror. Bending losses are minimized by putting both the transmitting and receiving fibers in close contact, thus forming a curvature of equal radius.

Static displacement of the mirror is achieved by mounting it on a micrometer translation stage. The distance between the fiber optic probe and the mirror is varied in successive steps of 50 μm and the voltage which represents the optical power is measured against the corresponding change in the translation stage. The optical power is then compared to the directly transmitted power from the transmitting fiber using the same light source. In this experiment, the modulated light source is used in conjunction with a lock-in amplifier to reduce the dc drift and interference of ambient stray light.

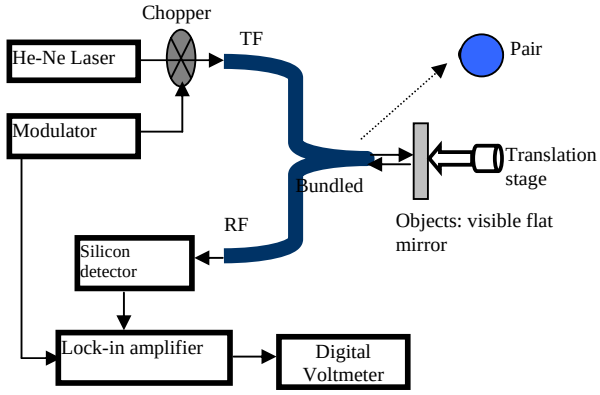

Fig. 3. Experimental setup of fiber optic displacement sensor. (TF: Transmitting fiber, RF: receiving fiber).

4. Results and discussion

The theoretical result in Eq. 9 is presented graphically and compared with an experimental result in Fig. 4. The plotted graph shows the normalized collected output power versus the normalized distance. Both curves exhibit a maximum with a steep front slope and back slope which follows an almost inverse square law relationship for the output power against a displacement distance. At h = 0, the plotted optical power does not equal to zero as expected. This is true for both the theoretical and experimental results, but more pronounced in the experimental results. This is due to the Gaussian beam truncation effect caused by the opaque outer jacket that covers the transmitting fiber and consequently prevents the light cone from reaching the receiving core. When the displacement is increased, the size of the reflected cone of light at the

plane of the fiber increases and starts overlapping with the receiving cores, leading to a small output power. A further increase in the displacement leads to larger overlapping which results in a further increase in the output power. However, after reaching the saturation region, the output power starts decreasing for larger displacements. This is due to the large increase in the size of the light cone and the subsequent decrease in the power density. The maximum normalized output power is obtained at a displacement distance of 1050 μm and 1750 μm with the theoretical and experimental approaches respectively.

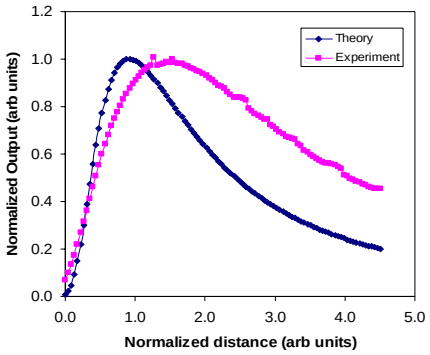

Fig. 4. Normalized Output versus normalized distance.

Both the theoretical slope and experimental slope curves show a good linearity as shown in Fig. 5 with a certain regions exhibits linearity of more than 99%. For the front slopes, the high linearity areas are obtained at a normalized displacement of 0.13 ~ 0.61 (corresponding to a displacement of 150 -700 μm) for the theoretical approach and 0.09 ~ 0.79 (corresponding to a displacement 100-900 μm) for the experimental result. On the other hand, the back slopes show a high linearity in the range of 1.14 ~ 2.15 (corresponding to a displacement of 1300~2450 μm) for the theoretical results and 1.80 ~ 3.59 (correspond with normalized displacement of 2050~4100 μm) for the experimental result. The sensitivity and linearity of both the front and back slopes of Fig. 5 are summarized in Table 1. According to Eq. 11, zero sensitivity occurs for $\zeta = \sqrt{8}$ when P_N reaches its peak. The sensitivity is positive on the front slope and negative on the back slope.

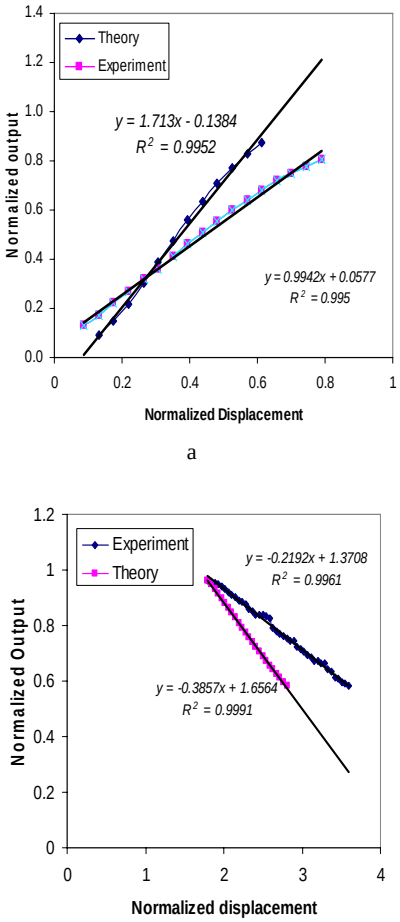

Fig. 5. Linearity range and sensitivity of the sensor for (a) the front slope and (b) the back slope.

Table 1. Comparison of the performance of the sensor with theoretical and experimental approaches.

Methods	The front slope			The back slope		
	Sensitivity	Linearity range		Sensitivity	Linearity range	
		Normalized displacement, h_N	Displacement (μm)		Normalized displacement, h_N	Displacement (μm)
Theoretical	1.7130	0.4821 (0.1314~0.6135)	550 (150~700)	0.3857	1.0080 (1.1394~2.1474)	1150 (1300~2450)
Experimental	0.9942	0.7012 (0.0876~0.7888)	800 (100~900)	0.2192	1.7968 (1.7968~ 3.5936)	2050 (2050~4100)

The fiber bundled sensor shows a longer linear range of 800 μm and 2050 μm for both the front and back slopes respectively as determined experimentally with a lower sensitivity compared to theoretical value. On the front slope the sensitivities are obtained at 1.71 and 1.0 mW/μm for the theoretical and experimental approaches respectively, while on the back slope the sensitivities are 0.38 and 0.22 mW/μm for theoretical and experimental

approaches respectively, which is smaller than the front slope. This discrepancy in theoretical and experimental values is due to neglecting the Gaussian beam truncation effects in our simple theoretical model. As indicated by the above results, we can conclude that the front slope is highly sensitive and useful for close distance targets while the back slope is less sensitive and useful for large displacement movements. The experimental results are capable of offering quantitative guidance for the design and implementation of the displacement sensor. This sensor has many potential applications in various industries such as automated monitoring control, position control and micro-displacement sensor in the hazardous regions.

5. Conclusions

A bundled fiber based optical displacement sensor is demonstrated using both a theoretical and experimental approach. The sensor uses a pair type bundled fiber in conjunction with an intensity modulation technique to measure the displacement between the mirror and bundled fiber's end. Both the experimental and theoretical results exhibit the same type of characteristic features; an initial increase of the optical power as distance starts to increase, followed by a slow falling decrease in power for higher distances. The front slope sensitivities are obtained at 1.71 and 1.0 mW/μm for the theoretical and experimental approaches, respectively, while the back slope sensitivities are 0.38 and 0.22 mW/μm for the theoretical and experimental approaches, respectively, which is smaller than the front slope. This discrepancy in theoretical and experimental values is due to the neglecting of the effect of Gaussian beam truncation in our theoretical model. The front slope is highly sensitive and useful for close distance targets while the back slope is less sensitive and useful for large displacement movements.

References

[1] S. Nalwa, Polymer optical fibres. California: American Scientific Publishers; 2004.
[2] Vijay K. Kulkarini, Anadkumar S. Lalasangi, I. I. Pattanashetti, U. S. Raikar, J. Optoelectron. Adv. Mater. **8**, 1610-1612 (2006).
[3] R. C. Spooncer, C. Butler, B. E. Jones, Opt Eng. **31**, 1632-1637 (1992).
[4] B. Culshaw, J. Dakin, Optical Fiber Sensors-Systems and Applications, Norwood, MA: Artech, 1989.
[5] P. LoPresti, W. Finn, Applied Optics **37**, 3426–3431 (1998).
[6] H. Gnewuch, N. N. Puscas, D. A. Jackson, A. Gh. Podoleanu, J. Optoelectron. Adv. Mater. **8**(1), 387 (2006).
[7] J. B. Faria, "A theoretical analysis of the bifurcated fiber bundle displacement sensor," IEEE Transactions on instrumentation and measurement, **47**, 742-747 (1998).

*Corresponding author: yasin@unair.ac.id